Journal of Machine Engineering, 2025, Vol. 25 ISSN 1895-7595 (Print) ISSN 2391-8071 (Online)

Received: 24 July 2025 / Accepted: 08 November 2025 / Published online: 27 November 2025

discharge frame, fatigue strength, S-N curve, fatigue

Dung Nguyen TIEN¹, Tung Nguyen ANH¹, Got Hoang VAN¹, Cuong Van NGUYEN^{2*}

INVESTIGATION OF THE FATIGUE BEHAVIOR OF THE DISCHARGE FRAME IN ELECTROSTATIC PRECIPITATORS UNDER SYMMETRIC CYCLIC LOADING

The discharge frame is a vital structural component of electrostatic precipitators (ESPs) and is frequently subjected to fully reversed cyclic loading from the rapping system. Because direct fatigue testing of the actual frame is impractical, this study proposes an indirect method to estimate its fatigue limit using experimental data from standard SS400 steel specimens combined with correction factors reflecting geometry, size, surface condition, and stress concentration. The fatigue tests established the S–N curve with parameters m=8.43 and C=26.05. The calculated fatigue limit of the discharge frame is significantly lower than that of the standard specimen, highlighting the effects of real structural conditions. The proposed approach provides a simple and effective tool for estimating the fatigue strength of large industrial components where direct testing or complex numerical analysis is not feasible.

1. INTRODUCTION

The electrostatic precipitator (ESP) operates on the principle of generating a strong electric field by applying a high-voltage direct current (ranging from several tens to several hundreds of kilovolts) to the electrode system. As the dust-laden gas stream passes through the precipitation chamber, the discharge electrodes ionize the dust particles, imparting a negative charge to them. These charged particles are then attracted to and deposited on the positively charged collecting plates [1–3]. The most critical component of the ESP is the precipitation chamber, which comprises a frame-type discharge electrode assembly equipped with sharp pins to ionize dust particles, and collecting plates to capture them [4].

During operation, dust gradually accumulates on the discharge electrodes and collecting plates. After a certain period of operation, it is necessary to clean these surfaces to maintain

¹ National Research Institute of Mechanical Engineering, Hanoi City 511309, Vietnam

² Faculty of Mechanical Engineering, University of Transport and Communications, Vietnam

^{*} E-mail: nguyencuong@utc.edu.vn https://doi.org/10.36897/jme/214078

the dust collection efficiency. A rapping system is employed to generate vibrations with appropriate acceleration and amplitude, detaching dust from the surfaces of the discharge electrodes and collecting plates [5].

According to previous studies, the minimum acceleration required to remove dust adhering to these plates is approximately 100 g, where g is the gravitational acceleration [4]. Therefore, parameters such as the frame dimensions, plate thickness, and plate material must be optimally designed, and the rapping hammer force must be properly calculated to generate the required acceleration throughout the system. The acceleration induced in the discharge electrodes and collecting plates also depends on the vibration frequency and the displacement generated by the rapping hammer [5, 6]. Under the action of the rapping hammer, the discharge frame is subjected to cyclic impact loading, which affects the fatigue strength of the frame.

The discharge frame of an electrostatic precipitator is subjected to cyclic impact loading generated by the rapping system during operation. This repeated loading induces material fatigue, which adversely affects the structural integrity and service life of the frame. Understanding the effects of cyclic impact forces on the fatigue behavior of the frame and its material properties, as well as establishing reliable methods for evaluating the fatigue strength, are therefore critical. Such an investigation enables an accurate assessment of the operational condition of the discharge frame and provides a foundation for developing engineering solutions to mitigate the risk of fatigue crack initiation, enhance fatigue resistance, and ultimately improve the reliability and efficiency of the electrostatic precipitator system.

There are multiple approaches available for evaluating the fatigue behaviour of structures subjected to variable amplitude loading (also known as spectrum loading). Among them, the most widely used is the Palmgren-Miner rule, with various modifications to account for real-world loading conditions [7–20]. In particular, fatigue life estimation is often conducted using the safe-life approach [21], in conjunction with the Linear Damage Rule (LDR) proposed by Palmgren [22] and Miner [23]. Due to its simplicity and ease of implementation, the Palmgren-Miner rule has become a standard tool in engineering fatigue analysis. This method also has several significant limitations that must be considered in practical applications [24]. A key shortcoming is its assumption that fatigue damage accumulates linearly and is independent of the loading sequence. In reality, many metallic materials display nonlinear fatigue damage evolution, which is highly dependent on both the stress amplitude and the order in which loads are applied [25]. Additionally, the Miner rule assumes that the fatigue limit is a fixed material constant, regardless of loading conditions. In contrast, numerous studies have shown that the actual fatigue limit may vary significantly with the stress amplitude history, making load sequence effects a critical factor in fatigue life prediction [26].

However, existing fatigue life prediction methods, such as the Palmgren–Miner rule, have notable limitations in accounting for nonlinear damage accumulation and load sequence effects. In electrostatic precipitators, the discharge frame is subjected to cyclic impact loads from the rapping system, making fatigue a critical concern. Direct fatigue testing of the frame is costly and impractical, while standard methods often neglect the combined effects of geometry, surface condition, and size.

This paper presents an efficient approach for estimating the fatigue limit of the discharge electrode frame under fully reversed cyclic loading, using standard SS400 steel specimen data and appropriate correction factors. The material employed, SS400 structural steel, is a widely used low-carbon steel defined in the Japanese Industrial Standard JIS G3101. It exhibits good weldability, machinability, and moderate strength, with typical mechanical properties including a yield strength of 245–250 MPa and an ultimate tensile strength of 400–510 MPa. Due to its high ductility and stable behavior under cyclic stress, SS400 is well suited for fatigue and structural reliability investigations. The proposed method provides a robust basis for improving design accuracy, enhancing fatigue resistance, and ensuring the operational reliability of electrostatic precipitator frames.

2. MATERIALS AND METHODS

2.1. THEORETICAL BASIS FOR DETERMINING THE FATIGUE LIMIT OF THE DISCHARGE FRAME IN ELECTROSTATIC PRECIPITATORS

Let σ de note the principal stress. The relationship between the number of stress cycles N and the magnitude of the principal stress in the discharge frame can be described by the following equation:

$$\sigma^m.N = 10^C \tag{1}$$

where m and C are the slope and intercept of the fatigue curve, respectively.

Currently, several indirect methods are available to determine the fatigue characteristics of structural components based on standard specimen data. The essence of these methods is founded on the brittle fracture hypothesis [27, 28]. The fatigue limit of the discharge frame is determined through standard specimens under fully-reversed cyclic loading conditions [27]:

$$\sigma_{-1D} = \frac{\bar{\sigma}_{-1} K_V K_A}{\frac{2K_t}{1 + \theta^{-v} \sigma} + \frac{1}{K_F} - 1} \tag{2}$$

where: $\bar{\sigma}_{-1}$ - Medium value of the endurance limit; K_V - Coefficient of a effect of surface hardening; K_A - Coefficient of anisotropy; K_F - Coefficient of a surface roughness; K_t - Stress concentration (theoretical) [26]. For components with complex geometries, the stress concentration factor K_t is determined using methods of the theory of elasticity or the finite element method (FEM).

 v_{σ} – the size sensitivity factor of the material to stress concentration, determined based on the fatigue fracture similarity equation [29]. The approximate value of v_{σ} can be calculated using the adjustment formula (for $\sigma_u \leq 1800MPa$) as follows:

$$v_{\sigma} = 0.2 - 0.0001.\,\sigma_u \tag{3}$$

 θ - the relative criterion of fatigue fracture similarity, determined by the following equation [28]:

$$\theta = \frac{L_D/\bar{G}_D}{L_O/\bar{G}_O} \tag{4}$$

where L_D – the length of the perimeter of the dangerous section or its part; L_o - the length of the perimeter of the critical zone of the standard specimen; \bar{G}_D , \bar{G}_o - the relative gradients of the first principal stress in the zone of its concentration for the part and the sample, respectively.

2.2. EXPERIMENTAL DETERMINATION OF THE FATIGUE CURVE OF THE DISCHARGE FRAME MATERIAL

The standard fatigue test specimen (Fig. 1) has a cylindrical geometry, machined on a CNC lathe and subsequently finished by precision grinding to achieve the required surface quality. Three identical specimens were tested in uniaxial tension using a United Calibration Corporation HFM500KN testing machine, and the average value from these three tests (Fig. 2) was recorded (Table 1). The material used for the specimens is SS400 carbon structural steel, which is equivalent to Q235 (GB/T 700, China) and A36 (ASTM, USA). This steel is widely used in mechanical structures due to its good weldability, moderate strength, and stable fatigue performance. Recent studies highlight that appropriate material selection should incorporate multi-criteria and objective weighting methods to ensure reliable performance in engineering applications [30-33], particularly for structural components subjected to cyclic loading.

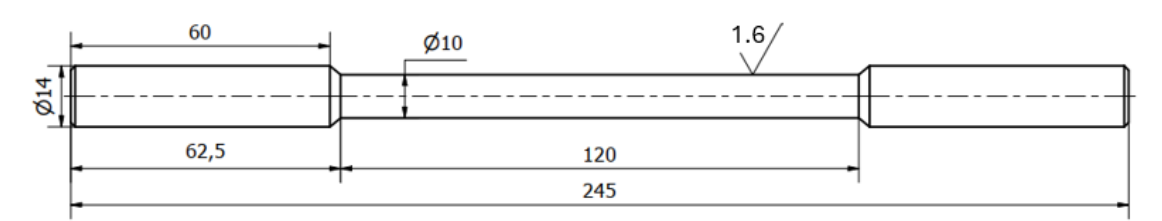


Fig 1. Dimensions of the standard specimen

The tensile test results of the standard specimens yield: $\sigma_{0.2}=328,17$ Mpa, ultimate tensile strength: $\sigma_u=418.44$ MPa. The approximate value of the size sensitivity factor v_σ can then be calculated by the empirical formula: $v_\sigma=0.2-0.0001$. $\sigma_u=0.158$.

| | | | • | 1 | | C | | |
|--|------|------|------|----------|---|----------|----------|------------|
| Load Cell S/N (0605553), Units (N) 120000 Preload Value (N) 500 | | | | | Crosshead Speed (mm/min) or Rate 5 Displacement Sensor XHD_100 (| | | |
| Test | Spec | D | L | Yield | Yield | Ultimate | Ultimate | Elongation |
| No | ID | (mm) | (mm) | Load (N) | Strength | Load | Strength | (%) |
| | | | | | (MPa) | (N) | (Mpa) | |
| 86 | 1 | 10 | 120 | 25.314 | 322.31 | 32.479 | 413.53 | 11.67 |
| 87 | 2 | 10 | 120 | 26.376 | 335.83 | 32.877 | 418.60 | 11.71 |
| 88 | 3 | 10 | 120 | 25.633 | 326.37 | 33.237 | 423.19 | 11.35 |
| Maan | | | | 25 774 | 328 17 | 32 864 | 118 11 | 11 58 |

Table 1. Mechanical properties obtained from tensile testing of standard specimens

To determine the mean fatigue limit σ_{-1} and the parameters m and C of the S–N curve under fully-reversed cyclic loading, a series of bending fatigue tests were performed on standard specimens. A total of eight standard cylindrical specimens made of SS400 carbon steel were prepared according to standard fatigue testing specifications. The specimens were machined on a CNC lathe to achieve the specified geometry and subsequently finished by precision grinding to obtain the required surface quality.

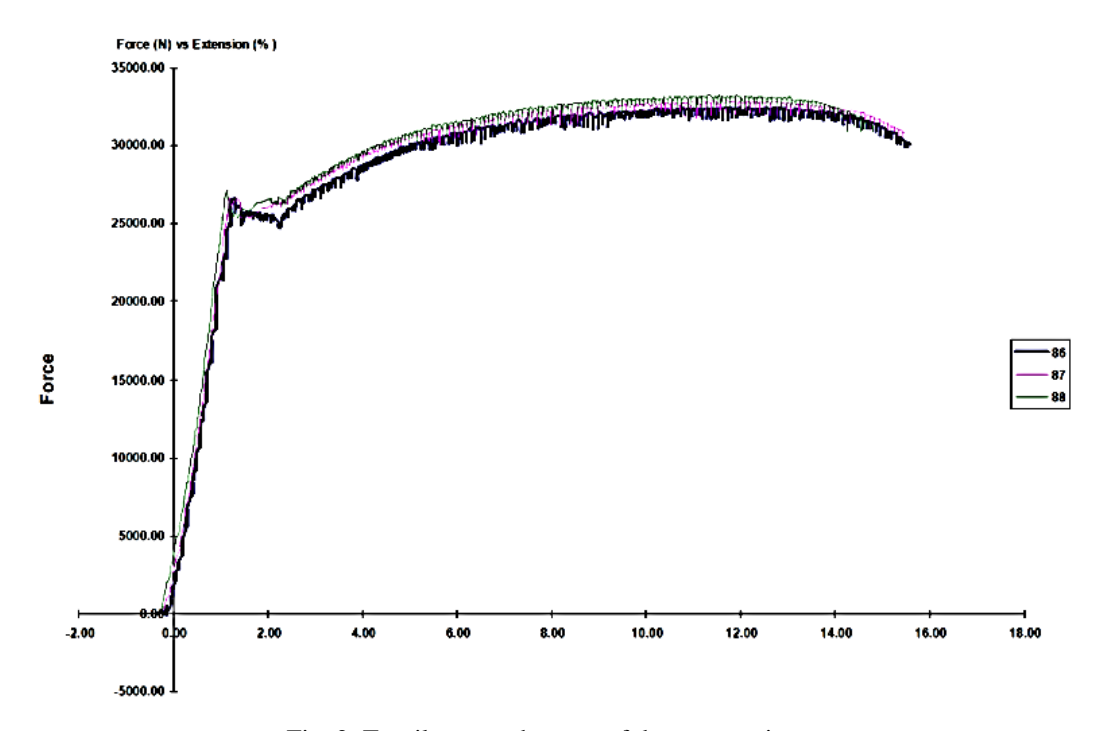


Fig. 2. Tensile strength curve of the test specimen

The fatigue tests were conducted under fully-reversed cyclic bending (R=-1) using a fatigue testing machine operating at a constant frequency. Each specimen was subjected to a predetermined stress amplitude until failure. During testing, the applied stress amplitude and the number of cycles to failure N_f were recorded for each specimen. These data points provided the experimental basis for constructing the S–N (stress versus number of cycles) curve and for calculating the fatigue strength parameters of the material. The load levels in Table 2 were selected based on the calibration of the bending test setup to generate stress amplitudes ranging from near the fatigue limit to about 0.6 UTS of the material. This range ensures both high-cycle and low-cycle fatigue regions are covered, allowing reliable determination of the S–N curve parameters. Table 2 summarizes the experimental data used for determining the mean fatigue limit and the parameters of the S–N curve.

The mean fatigue limit σ_{-1} is defined as the maximum stress amplitude that the material can sustain for at least 10^7 loading cycles without failure. Based on the data from specimens 7 and 8, the stress corresponding to $N = 10^7$ cycles is determined to be: $\sigma_{-1} = 181.3MPa$.

The fatigue behavior of the material is represented by the S–N curve, which is described using a logarithmic form:

$$logN = C - mlog\sigma (5)$$

Using the tabulated test results (Table 2), the parameters m and C were calculated as follows:

$$m = \frac{\log N_2 - \log N_1}{\log \sigma_1 - \log \sigma_2}; C = \log N_1 + m \log \sigma_1 \tag{6}$$

The calculated values of the parameters are: m = 8.43; C = 26.05

Accordingly, the S–N curve equation of the standard specimen under fully-reversed cyclic loading is expressed as:

$$logN = 26.05 - 8.43log\sigma \tag{7}$$

| Specimen | Load | Section moment of | Number of cycles to | Fatigue stress amplitude |
|----------|------|----------------------------|---------------------|--------------------------|
| | (kg) | inertia (cm ⁴) | failure N_f | (MPa) |
| 1 | 43 | 0.039263 | $6.57x10^5$ | 249.9 |
| 2 | 40 | 0.039263 | $9.98x10^{5}$ | 231.8 |
| 3 | 37 | 0.039263 | $2.09x10^6$ | 215.7 |
| 4 | 36 | 0.039263 | $2.40x10^6$ | 212.6 |
| 5 | 34 | 0.039263 | $4.62x10^6$ | 197.6 |
| 6 | 32 | 0.039263 | $7.90x10^6$ | 185.4 |
| 7 | 31 | 0.039263 | $1.00x10^7$ | 181.3 |
| 8 | 31 | 0.039263 | $1.00x10^7$ | 181.3 |

Table 2. Bending fatigue test results of SS400 steel specimens

Figure 3 shows the experimental S–N (Wöhler) curve of SS400 steel. The test results follow a clear logarithmic relation expressed by $\log N = 26.05 - 8.43\log \sigma$, with good agreement between the regression line and experimental points. The fatigue limit was determined to be approximately 181.9 MPa at $N = 10^7$ cycles, which is consistent with typical values for mild structural steels. This S–N curve provides a reliable basis for evaluating the fatigue behavior of the discharge frame material and serves as a reference for subsequent fatigue strength estimation

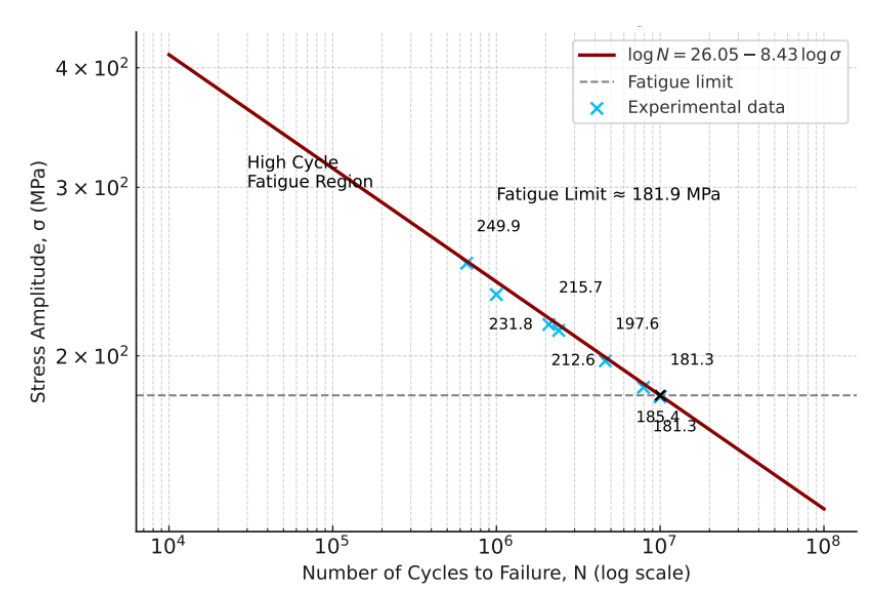


Fig. 3. S-N (Wöhler) curve of SS400 steel obtained from regression analysis and experimental data

3. RESULTS AND DISCUSSION

The general structure of the ESP system is illustrated in Fig. 4. The discharge frame (Fig. 5) is fabricated from SS400 carbon steel pipe with an outer diameter of D = 27.2 mm and wall thickness t = 2.8 mm. The calculated relative fatigue fracture similarity criterion was determined to be $\theta = 2.72$.

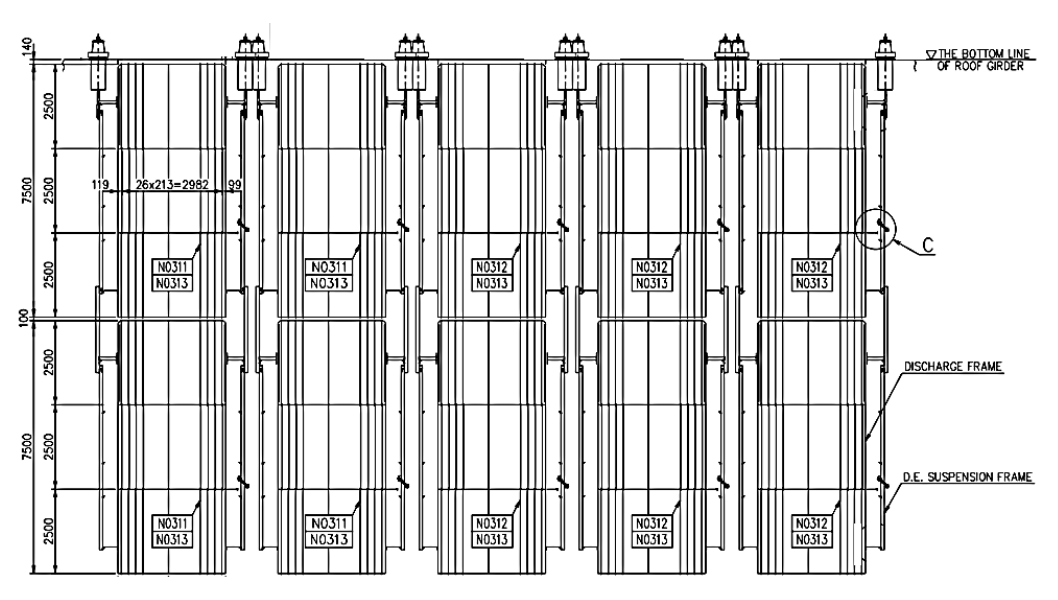


Fig. 4. Electrostatic precipitator, collecting plates, and rapping System

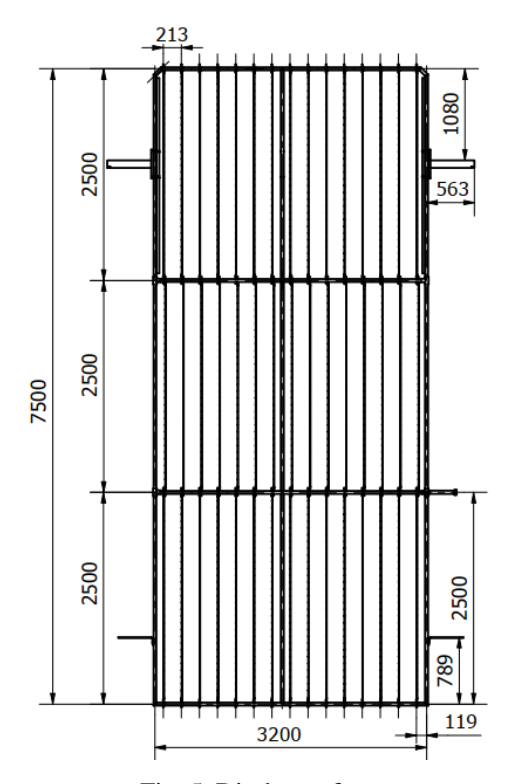


Fig. 5. Discharge frame

The transverse beams of the discharge frame are drilled to mount the discharge electrodes. The mass of the discharge frame is m_2 =280 kg. A rapping hammer is installed at the anvil position on the discharge frame with a detachable design. Based on the design and manufacturing method of the discharge frame, the following factors are determined: $K_t = 1.5$, $K_A = 1$, $K_F = 0.75$, $K_V = 1$ [34, 35].

By substituting these factors into equation (2), the fatigue limit of the discharge frame under fully-reversed cyclic loading is determined as: $\sigma_{-1D} = 92.86$ MPa The calculation results show that the actual fatigue limit of the discharge frame is $\sigma_{-1D} = 92.86$ MPa, which is significantly lower than the mean fatigue limit of the standard SS400 steel specimen $\sigma_{-1} = 181.3$ MPa. This discrepancy clearly reflects the influence of actual structural factors such as larger dimensions, geometric stress concentration, and surface condition.

The method for determining the fatigue limit of the discharge frame in this study is based on experimental data from standard specimens combined with correction factors, demonstrating its feasibility and effectiveness in situations where direct testing on the actual component is not possible. This approach utilizes reliable experimental results from standard specimens while incorporating correction factors that account for the effects of size, geometry, surface condition, and stress state of the actual structure.

Compared with recent fatigue models based on equivalent stress transformation, heat dissipation, or damage mechanics [9, 10, 16, 34], the present correction-factor-based approach provides a simpler and more practical estimation method suitable for industrial components such as electrostatic precipitator frames. The use of the generalized Weibull-type formula to describe the effect of relative size represents an improvement over traditional methods relying solely on conventional size factors, capturing the statistical nature of fatigue failure and the nonlinear degradation of the fatigue limit as the component size increases.

However, this method also reveals certain limitations. The accuracy of the results heavily depends on the reliability of the correction factors, which are often obtained from tables or estimated theoretically and may not fully reflect the actual characteristics of each specific component. In addition, the model assumes a purely fully-reversed cyclic loading condition, whereas in practice, more complex loading scenarios may occur.

This method is suitable for quickly estimating the fatigue limit of actual components during the preliminary design stage or when direct testing is not yet feasible. It also provides an assessment of the reduction in fatigue strength due to geometric and surface factors. However, to improve the reliability of the design, it is recommended to validate the results through numerical simulation (FEM) or experimental testing on equivalent specimens.

4. CONCLUSIONS

This paper presented a method for determining the actual fatigue limit of the discharge frame under fully-reversed cyclic loading, based on experimental data from standard SS400 steel specimens combined with correction factors that account for the effects of geometry, size, surface condition, and actual stress state.

The calculation results show that the actual fatigue limit of the discharge frame is $\sigma_{-1D} = 92.86$ MPa, which is significantly lower than that of the standard specimen. This reduction clearly reflects the combined influence of stress concentration, larger dimensions, and surface quality of the actual structure compared to the standard specimen.

The methodology can be extended to other structural steels and loading conditions, offering a useful reference for the design and durability evaluation of mechanical structures operating under cyclic loads.

REFERENCES

- [1] MIZUNO A., 2000, Electrostatic Precipitation, IEEE Trans. Dielectr. Electr. Insul., 7/5, 615-624, https://doi.org/10.1109/94.879357.
- [2] MCLEAN K.J., 1988, *Electrostatic Precipitators*, IEE Proc. A, 135/6, 347–361, https://doi.org/10.1049/ip-a-1.1988.0056.
- [3] CHIANG P.C., GAO X., 2022, *Electrostatic Precipitator*, Air Pollution Control and Design. Springer, Singapore, https://doi.org/10.1007/978-981-13-7488-3_19.
- [4] NEYESTANAK A.A.L., NAZARI S., IMAM A., AGHANAJAFI C., 2014, Fatigue Durability Analysis of Collecting Rapping System in Electrostatic Precipitators Under Impact Loading, Adv. Mater. Sci. Eng., 136059, https://doi.org/10.1155/2014/136059.
- [5] GUDANOV I.S., LEBEDEV A.E., VATAGIN A.A., 2022, *Modernization of a High-Performance Electrostatic Precipitator*, Chem. Petrol. Eng., 57, 963–965, https://doi.org/10.1007/s10556-022-01031-1.
- [6] PARKER K., 2007, *Electrical Operation of Electrostatic Precipitators*, Institution of Engineering and Technology, London.
- [7] BAUMGARTNER J., BREITENBERGER M., SONSINO C.M., 2024, Required Fatigue Strength (RFS) a Simple Concept for Determining an Equivalent Stress Range Indicating the Necessary Minimum Joint Quality, Weld World, 68, 3177–3194, https://doi.org/10.1007/s40194-024-01820-7.
- [8] SONSINO C.M., BAUMGARTNER J., BREITENBERGER M., 2022, Equivalent Stress Concepts for Transforming Variable Amplitude Into Constant Amplitude Loading and Consequences for Design and Durability Approval, Int. J. Fatigue, 162, 106949, https://doi.org/10.1016/j.ijfatigue.2022.106949.
- [9] SONSINO C.M., RENNERT R., 2023, Comparison of Two Equivalent Stress Methods Based nn Cumulative Damage Adjustment and on a Consistent Fatigue Strength Reduction for Transforming Variable Into Constant Amplitude Loading, Mater. Test., 65/5, 662-683, https://doi.org/10.1515/mt-2022-0373.
- [10] PELIZZONI S., RICOTTA M., CAMPAGNOLO A., MENEGHETTI G., 2024, Analysis of the Uniaxial Fatigue Behaviour of 42crmo4 Q&T Steel Specimens Extracted from a Marine Engine Connecting Rod Using the Heat Dissipation Approach, Procedia Struct. Integr., 57, 404-410, https://doi.org/10.1016/j.prostr.2024.03.043.
- [11] BRNIC J., BRCIC M., BALOS S., VUKELIC G., KRSCANSKI S., MILUTINOVIC M., DRAMICANIN M., 2021, S235JRC+C Steel Response Analysis Subjected to Uniaxial Stress Tests in the Area of High Temperatures and Material Fatigue, Sustainability, 13/10, 5675, https://doi.org/10.3390/su13105675.
- [12] SANTECCHIA E., HAMOUDA A.M.S., MUSHARAVATI F., et al., 2016, A Review on Fatigue Life Prediction Methods for Metals, Adv. Mater. Sci. Eng., 2016, 9573524, https://doi.org/10.1155/2016/9573524.
- [13] ZALNEZHAD E., SARHAN A.A.D.M., HAMDI M., 2012, Prediction of TiN Coating Adhesion Strength on Aerospace AL7075-T6 Alloy Using Fuzzy Rule Based System, Int. J. Precis. Eng. Manuf., 13, 1453–1459. https://doi.org/10.1007/s12541-012-0191-3.
- [14] KREISER D., JIA S.X., HAN J.J., DHANASEKAR M., 2007, A Nonlinear Damage Accumulation Model for Shakedown Failure, Int. J. Fatigue, 29/8, 1523–1530, https://doi.org/10.1016/j.ijfatigue.2006.10.023.
- [15] MAKKONEN M., 2009, *Predicting the Total Fatigue Life in Metals*, Int. J. Fatigue, 31/7, 1163-1175, https://doi.org/10.1016/j.ijfatigue.2008.12.008.
- [16] ZHU S.-P., HUANG H.-Z., 2010, A Generalized Frequency Separation-Strain Energy Damage Function Model for Low Cycle Fatigue-Creep Life Prediction, Fatigue Fract. Eng. Mater. Struct., 33/4, 227–237, https://doi.org/10.1111/j.1460-2695.2009.01431.x.

- [17] KUANG Y., WANG G., TIAN R., HE C., FAN F., LI W., PANG W., 2025, A Fatigue Life Prediction Model of Stud Based on Damage Mechanics, Fatigue Fract. Eng. Mater. Struct., 48, 2618–2632, https://doi.org/10.1111/ffe.14629.
- [18] GAO H.Y., ZUO F.J., L. Z.Q., 2015, Residual Life Prediction Based on Nonlinear Fatigue Damage Accumulation Model, J. Shanghai Jiaotong Univ. (Sci.), 20, 449–453, https://doi.org/10.1007/s12204-015-1647-2.
- [19] AYOUB G., NAIT-ABDELAZIZ M., ZAIRI F., GLOAGUEN J.M., 2010, Multiaxial Fatigue Life Prediction of Rubber-Like Materials Using the Continuum Damage Mechanics Approach, Procedia Eng., 2/1, 985-993, https://doi.org/10.1016/j.proeng.2010.03.107.
- [20] ZHANG Y., WANG N., ZHOU J., WANG H., TANG L., ZHANG Y., ZHANG Z., 2024, Remaining Fatigue Life Prediction of Additively Manufactured Inconel 718 Alloy Based on In-Situ SEM and Deep Learning, Eng. Fail. Anal., 163A, 108440, https://doi.org/10.1016/j.engfailanal.2024.108440.
- [21] SURESH S., 1998, Fatigue of Materials, 2nd Ed., Cambridge University Press, Cambridge.
- [22] PALMGREN A.G., 1924, Life Length of Roller Bearings, Z. Ver. Dtsch. Ing., 14, 339–341.
- [23] MINER M.A., 1945, Cumulative Damage in Fatigue, J. Appl. Mech., 3, 159–164.
- [24] JSCHIJVE J., 2001, Fatigue of Structures and Materials, Springer, Dordrecht.
- [25] VARVANI-FARAHANI A., SHARMA M., KIANOUSH M.R., 2005, Fatigue Damage Analysis and Life Assessment Under Variable Amplitude Loading Conditions, Mater. Sci. Eng. A, 403, 42–47, https://doi.org/10.1016/j.msea.2005.05.018.
- [26] XI X.L., SONGLIN Z., 2009, Strengthening and Damaging Under Low-Amplitude Loads Below the Fatigue Limit, Int. J. Fatigue, 31/2, 341–345, https://doi.org/10.1016/j.ijfatigue.2008.08.004.
- [27] KOGAEV V.P., MAKHUTOV N.A., GUSENKOV A.P., 1985, Calculations of Machine Elements and Structures for Strength and Durability: Handbook, Mashinostroyeniye Publ., Moscow (in Russian).
- [28] GOST 25.504-82, Calculations and Strength Tests. Methods for Calculating Fatigue Resistance Characteristics, Moscow (in Russian).
- [29] ZHANG W., WANG Q., LI X., HE J., 2016, A Simple Fatigue Life Prediction Algorithm Using the Modified NASGRO Equation, Math. Probl. Eng., 04298507, https://doi.org/10.1155/2016/4298507.
- [30] DUA T.V., DUC D.V., BAO N.C., TRUNG D.D., 2024, Integration of Objective Weighting Methods for Criteria and MCDM Methods: Application in Material Selection, EUREKA: Physics and Engineering, 2, 131–148. https://doi.org/10.21303/2461-4262.2024.003171.
- [31] DO D.T., NAZLI E., VO T.N.U., 2024, *Cylinder and Piston: Material Selection in the Design Phase*, Journal of Applied Engineering Science, 22/4, 789–803. https://doi.org/10.5937/jaes0-52884.
- [32] TRUNG D.D., THINH H.X., HA L.D., 2022, Comparison of the RAFSI and PIV Method in Multi-Criteria Decision Making: Application to Turning Processes, Int. J. Metrol. Qual. Eng. 13, 14, https://doi.org/10.1051/ijmqe/2022014.
- [33] CUONG N.V., KHANH N.L., 2021, Parameter Selection to Ensure Multi-Criteria Optimization of the Taguchi Method Combined with the Data Envelopment Analysis-Based Ranking Method when Milling SCM440 Steel, Engineering, Technology & Applied Science Research., 11, 5,7551–7557. https://doi.org/10.48084/etasr.4315.
- [34] PILKEY W.D., 1997, Peterson's Stress Concentration Factors, 2nd ed., Wiley, New York.
- [35] JIMENEZ-ALFARO S., MARTINEZ-PANEDA E., 2025, A Computational Framework for Predicting the Effect of Surface Roughness in Fatigue, Int. J. Fatigue, 199, 109044. https://doi.org/10.1016/j.ijfatigue.2025.109044.